Direct sequencing of total *S. cerevisiae* tRNAs by LC-MS/MS

Joshua D. Jones[1], Kaley M. Simcox[1], Robert T. Kennedy[1], Kristin S. Koutmou[1,*]

[1]University of Michigan, Department of Chemistry. 930 N University, Ann Arbor, MI 48109, *corresponding author (734) 764-5650, kkoutmou@umich.edu

Keywords: tRNA modifications, RNA sequencing, LC-MS/MS

Abstract

Among RNAs, transfer RNAs (tRNAs) contain the widest variety of abundant post-transcriptional chemical modifications. These modifications are crucial for tRNAs to participate in protein synthesis, promoting proper tRNA structure and aminoacylation, facilitating anticodon:codon recognition, and ensuring the reading frame maintenance of the ribosome. While tRNA modifications were long thought to be stoichiometric, it is becoming increasingly apparent that these modifications can change dynamically in response to the cellular environment. The ability to broadly characterize the fluctuating tRNA modification landscape will be essential for establishing the molecular level contributions of individual sites of tRNA modification. The locations of modifications within individual tRNA sequences can be mapped using liquid chromatography coupled to tandem mass spectrometry (LC-MS/MS). In this approach, a single tRNA species is purified, treated with ribonucleases and the resulting single-stranded RNA products are subject to LC-MS/MS analysis. The application of LC-MS/MS to study tRNAs is limited by the necessity of analyzing one tRNA at a time because the digestion of total tRNA mixtures by commercially available ribonucleases produces many short digestion products unable to be uniquely mapped back to a single site within a tRNA. We overcame these limitations by taking advantage of the highly structured nature of tRNAs to prevent the full digestion by single-stranded RNA specific ribonucleases. Folding total tRNA prior to digestion allowed us to sequence *S. cerevisiae* tRNAs with up to 97% sequence coverage for individual tRNA species by LC-MS/MS. This method presents a robust avenue for directly detecting the distribution of modifications in total tRNAs.

Introduction

RNAs can include over 150 enzymatically incorporated post-transcriptional chemical modifications (Boccaletto et al. 2018; McCown et al. 2020). These modifications are found on every class of RNAs, including ribosomal RNAs (rRNAs), transfer RNAs (tRNAs) and messenger RNAs (mRNAs), where they impact nearly every stage of the RNA lifecycle (Jones et al. 2020; McCown et al. 2020). tRNAs have the most diverse modification landscape of any class of RNA molecules, with modifications playing a multitude of roles that vary depending upon their position within the tRNA. For example, modifications near the tRNA anticodon commonly modulate decoding and frame maintenance, while modifications at other locations within tRNAs contribute to stability, folding, and ribosome-tRNA interactions (Zhang et al. 2022; Jackman and Alfonzo 2013). tRNA modifications were originally believed to be stoichiometric and static, however recent evidence suggest that the tRNA modification landscape is dynamically altered under stress and disease, such as mitochondrial disease and type 2 diabetes (Chan et al. 2010, 2012; Yoluç et al. 2021; Asano et al. 2018; Ishida et al. 2011; Alings et al. 2015; Suzuki 2021; Huber et al. 2019).

In light of these observations, new methodologies for the rapid and robust characterization of the tRNA modification landscape are of significant interest. For over 20 years the modified sites of highly purified individual tRNAs have been identified using bottom-up RNA sequencing (Kowalak et al. 1993; Jora et al. 2019; Suzuki et al. 2020; Suzuki and Suzuki 2007), where modified sites are identified by a mass shift detected in precursor and product ion scans. However, long intact RNAs remain difficult to robustly sequence by direct MS/MS (Taucher and Breuker 2012; Crittenden et al. 2023; Taucher and Breuker 2010). Consequently, RNAs are commonly digested using ribonucleases to smaller fragments that can be sequenced by MS/MS, analogous to bottom-up proteomics. While this process has enabled the sequencing of purified individual tRNAs (Suzuki et al. 2020; Addepalli and Limbach 2016), rRNAs (Popova and Williamson 2014; Taoka et al. 2018, 2016, 2015), and therapeutic RNAs (e.g., CRISPR guide RNAs, therapeutic mRNAs, siRNA) (Jiang et al. 2019; Vanhinsbergh et al. 2022; Goyon et al. 2021, 2022; Jones et al. 2023b), full sequence coverage of RNA mixtures is difficult to achieve because of the formation of nonunique digestion products that do not map back to a single

site. As a result, bottom-up RNA sequencing of tRNAs requires the purification and analysis with multiple ribonucleases for each individual tRNA to obtain full sequence coverage. The limitation of characterizing a single tRNA at a time has long impeded the comprehensive interrogation of the tRNA modification landscape and its dynamics by bottom-up RNA sequencing.

There is substantial interest in developing LC-MS/MS approaches to directly sequence total tRNA pools, viral RNA genomes, and purified highly modified RNA species (e.g., mRNA vaccines and therapeutics). Current methods for sequencing these more complex samples employ an array of orthogonal enzymes that provide overlapping digestion products and full sequence coverage, including RNase T1 (G-specific) (Jiang et al. 2019; Ross et al. 2016; Addepalli and Limbach 2016; Wetzel and Limbach 2013; Popova and Williamson 2014; Pomerantz and McCloskey 2005; Thakur et al. 2020; Vanhinsbergh et al. 2022; Ohira et al. 2022; Goyon et al. 2021; Suzuki et al. 2020; Kimura et al. 2020; Wein et al. 2020; Taoka et al. 2018, 2016, 2015), RNase A (pyrimidine specific) (Popova and Williamson 2014; Ohira et al. 2022; Kimura et al. 2020; Taoka et al. 2018, 2016; Goyon et al. 2021; Suzuki et al. 2020), cusativin (C-specific) (Thakur et al. 2020; Addepalli et al. 2017), RNase MC1 (U-specific) (Addepalli et al. 2015; Thakur et al. 2020), colicin E5 (GU-specific) (Jiang et al. 2019), and RNase H (DNA-RNA duplex regions) (Taoka et al. 2018, 2016, 2015; Yan et al. 2021). This process has enabled the sequencing of a multitude of RNA species, including the adaptation to more complex samples with total tRNA (Thakur et al. 2020), ribosomal RNA (Taoka et al. 2018, 2016, 2015), and long therapeutic mRNAs (Jiang et al. 2019). However, many key enzymes are not commercially available (e.g., cusativin, RNase MC1, colicin E5) and are difficult to obtain because they cleave endogenous RNAs *in vivo,* making them toxic to the cells used for their production. While the partial digestion of purified mRNAs by RNase T1 has been used as an alternative to orthogonal digestions to improve LC-MS/MS sequencing of long mRNAs (Vanhinsbergh et al. 2022), partial digestions produce a low abundance and diverse oligonucleotide digestion product mixture that reduces MS/MS signal intensity and complicates data analysis.

To circumvent these limitations, we drew inspiration from the foundational work over 40 years ago to structurally map RNAs using single stranded specific RNases (Lockard and Kumar 1981; Wurst et al. 1978; Donis-Keller et al. 1977). Analogously, we leveraged the inherent stability of tRNA secondary structures to selectively restrain ribonuclease digestion to single-stranded regions. Digestion of folded tRNAs produces longer and more unique oligonucleotides, facilitating bottom-up RNA sequencing of complex RNA mixtures using solely commercial, readily available enzymes (RNase T1 and RNase A). We found that this adaptation primarily limits ribonuclease cleavage to stem loops and more dynamic tRNA regions (e.g., variable loops) and consequently enhances the sequence coverage of total tRNA by bottom-up RNA sequencing. Overall, this process provides a selective and reproducible pipeline to produce longer and more unique oligonucleotide digestion products prior to LC-MS/MS sequencing, enabling 60-90% sequence coverage for most tRNA with only commercial ribonucleases by LC-MS/MS.

Results and discussion

tRNA secondary structure protects against ribonuclease digestion and reduces the complexity of digested total tRNA mixtures

tRNA structures are essential both for their biological function in protein synthesis, and to prevent their degradation by endogenous ribonucleases *in vivo*. The refolding of tRNA is commonplace prior to *in vitro* biochemical analysis to ensure proper tRNA structure for related investigations. We utilized an analogous protocol to fold total tRNA prior to ribonuclease digestion using both monovalent (sodium or potassium) and divalent (magnesium) cations to stabilize tRNA structure. Since tRNA contain significant secondary structure, we posited that digestion by single stranded specific ribonucleases will be limited to the single stranded stem loops of the tRNA (D-loop, anticodon stem loop, and T-loop) **(Figure 1A)**. Consequently, longer and more specific oligonucleotide digestion products would be produced compared to complete ribonuclease digestions of total tRNA.

We initially tested this approach using single stranded specific RNase T1 to digest folded *S. cerevisiae* total tRNA, which provides a diverse tRNA landscape of broad lengths and post-transcriptional modifications. tRNA structure and dynamics is highly dependent on temperature (Yamagami et al. 2022); thus, we first characterized the temperature dependence of RNase T1 digestion of folded tRNAs. We compared the folded tRNA digestions to a complete RNase T1 digestion condition commonly employed for bottom-up RNA sequencing (100 U/µg in 220 mM ammonium acetate at 37℃). As expected, under standard digestion temperatures (37℃), the tRNA is not fully protected against RNase T1 digestion (i.e., 100 U RNase T1 per µg of RNA still fully digests the folded total tRNA, **Supplemental Figure S1)**. Thus, *S. cerevisiae* tRNA is likely dynamic, exhibiting significant structural breathing at 37℃ despite the presence of monovalent and divalent cations, possibly suggesting that a population of tRNA is partially unfolded despite the melting temperature of *S. cerevisiae* tRNA being 76℃ (Watanabe et al. 2013). This is perhaps unsurprising considering 37℃ is a heat shock condition for *S. cerevisiae*. However, as the digestion temperature is decreased to 30℃ and 25℃, tRNA folding provides more protection against RNase T1 digestion regardless of the enzyme

concentration utilized in the reaction **(Supplemental Figure S1)**. This is likely due to the reduction in tRNA dynamics. We found that 25℃ provided the most consistent digestion conditions independent of the enzyme concentration utilized in the reaction; this temperature was selected for use in our study.

In addition to temperature, tRNA structure is highly dependent on the presence of divalent cations. tRNAs can contain up to six Mg^{2+}/phosphate interactions that stabilize proper tertiary structure (Schauss et al. 2021). Our data corroborate these findings, where the selective protection against single stranded specific RNase T1 digestions varies with divalent cation concentration. When no Mg^{2+} is added into the digestions, RNase T1 fully digests the total tRNA in both ammonium acetate (NH_4OAc) and 2-(N-morpholino)ethanesulfonic acid (MES) pH 6.0/potassium chloride buffers **(Figure 1B)**. However, when 20 mM Mg^{2+} is incorporated, the total tRNA spontaneously folds leading to the selective protection against RNase T1 digestions **(Figure 1B)**. RNase T1 is known to be inhibited by the presence of divalent cations; however, previous investigations have shown that denatured tRNAs are much more sensitive to RNase T1 digestion than folded tRNAs in similar quantities of Mg^{2+} (Adams et al. 1967). We find that this protection does not require the melting and slow cooling to form stable tRNA secondary structures; however, minor alterations in the oligonucleotide digestion product profile suggest a more diverse array of secondary structures is formed without reannealing the tRNA before the addition of Mg^{2+} **(Figure 1B)**. Together, this suggests that, as anticipated, Mg^{2+} is essential for stable folding of *S. cerevisiae* tRNA to produce longer RNase T1 oligonucleotide digestion products.

The standard cloverleaf secondary structure of tRNA should protect against digestion by single stranded specific ribonucleasesin the three tRNA stem loop regions. If our folded total tRNA digestions occur as anticipated, we reasoned that the resulting oligonucleotide digestion products would range from 15-20 nt if all three stem loops are cleaved, or 30-40 nt if a stem loop is missed (e.g., a stem loop does not contain a guanosine for RNase T1 digestions). Our results indicate that this is indeed the case, with the RNase digestion of folded total tRNAs primarily yielding oligonucleotide digestion products of the expected lengths **(Figure 1B)**. This conclusion is supported by liquid

chromatography coupled to UV absorbance detection (LC-UV), where less oligonucleotide signal for 20-30 nt oligonucleotides is observed relative to 14-20 nt and >30 nt oligonucleotides that correspond to digestion in the tRNA stem loops **(Figure 1C and 1D)**. Thus, tRNA secondary structure protects against RNase T1 digestion, resulting in longer digestion products that could facilitate the RNA LC-MS/MS sequencing. We predicted that the tRNA fragment lengths we obtained would be readily sequenced on the timescale of a UHPLC separation, since even longer oligonucleotide digestion products (≥ 40 nt) were previously sequenced during the bottom-up RNA sequencing of long purified messenger RNAs (Vanhinsbergh et al. 2022).

While folding tRNAs reduces the complexity of the digested total tRNA mixtures, it does not fully remove the production of short oligonucleotide digestion products **(Figure 1B and 1D)**. This suggests that tRNA remains modestly dynamic and maintains ribonuclease access to some cleavage sites present in double stranded regions. This effect is likely beneficial since we obtain both complete cleavage products and longer tRNA structure protection digestion products for analysis by LC-MS/MS sequencing. Together, digestion of folded total tRNA yields increases the fraction of longer oligonucleotide digestion products, leading to higher sequence coverages of complex total tRNA mixtures by bottom-up RNA sequencing.

Previously, partial ribonuclease digestions were used to produce longer and more specific digestion products to improve sequence coverage by bottom-up RNA sequencing (Vanhinsbergh et al. 2022). However, since the ribonuclease can digest anywhere throughout the RNA, partial digestions produce complex and diverse oligonucleotide digestion product mixtures, which reduce signal intensity and complicate data analysis. In contrast, our folded total tRNA digestions yield a more selective pool of longer oligonucleotide digestion products. We observe this where folded total tRNA digestions yield more specific longer oligonucleotide fragments compared to partial RNase T1 digestions, as seen by the sharper peaks for longer digestion products by LC-UV **(Supplemental Figure S2)**. Further, partial RNase T1 digestions produce a mixture of 3’ phosphate and 2’3’-cyclic phosphate digestion products (Vanhinsbergh et al. 2022). Here, we find that folded total tRNA RNase T1 digestions produce only 3’ digestion products

(Supplemental Figure S3), suggesting that the digestion goes to completion despite containing many missed cleavage sites. This further reduces the complexity of the digestion product pool while producing longer and more specific oligonucleotide fragments to facilitate sequencing by LC-MS/MS.

In addition to RNase T1, RNase A is a common single stranded specific ribonuclease for bottom-up RNA sequencing that cleaves at pyrimidine residues. We tested the ability of RNase A to cleave folded total tRNA and provide an orthogonal digestion to RNase T1 to increase downstream sequence coverage. Similar to RNase T1 digestions, we folded total tRNA in the presence of a monovalent cation and magnesium. Since RNase A requires high concentrations of NaCl (instead of KCl) to specifically target ssRNA, we replaced KCl with NaCl for this application (Ausubel 1987). Similar to RNase T1, tRNA secondary structure protects against RNase A digestion with these adaptations. RNase A demonstrated a different cleavage pattern than RNase T1, primarily generating oligonucleotide digestion products approximately half the size of a tRNA, likely corresponding to the cleavage in the anticodon stem loop **(Supplemental Figure S4)**.

Overall, tRNA secondary structure protects against single stranded specific RNase T1 and RNase A digestions, and digestion of folded total tRNAs results in the production of longer oligonucleotide digestion products. This simple change in digestion protocol is a key innovation because a primary limitation of bottom-up RNA sequencing of total tRNA and complex RNA mixtures has been the production of short, nonunique digestion products by commonplace ribonuclease digestions. This modification of previous digestion workflows could enhance attainable sequence coverages by bottom-up RNA sequencing without requiring orthogonal digestions from non-commercial enzymes or partial RNase digestions that result in arduous and non-robust data analysis, and limited sequence coverage.

Bottom-up RNA sequencing of S. cerevisiae total tRNA

Bottom-up RNA sequencing of complex RNA mixtures is hindered by the significant production of small, nonunique digestion products that do not map to a single

location. As a result, most applications have been limited to highly purified individual tRNAs. While bottom-up RNA sequencing can be applied to complex total tRNA pools (Puri et al. 2014; Hagelskamp et al. 2020; Cao and Limbach 2015; de Crécy-Lagard et al. 2020; Yu et al. 2019), this assay is generally used to confirm select modified positions previously identified by other sequencing methods, rather than fully sequencing the tRNA modification landscape. Recently, orthogonal enzymatic digestions were performed that provide more unique oligonucleotide digestion products and enable the deep sequencing of total *E. coli* tRNA mixtures by bottom-up RNA sequencing (Thakur et al. 2020). While powerful, the requirement of three orthogonal enzymes limits the accessibility of this process because it requires the expression and purification of non-commercially available toxic ribonucleases.

To facilitate total tRNA sequencing using exclusively commercial enzymes, we exploited tRNA structure to selectively protect against digestion by single stranded specific ribonucleases to produce longer oligonucleotide digestion products without the need for partial digestions, allowing us to sequence total *S. cerevisiae* tRNAs by LC-MS/MS (**Figures 1A, 2A, and 2B and Table 1**). We digested *S. cerevisiae* total tRNA using either RNase T1 or RNase A in either the unfolded or folded conformations. Further, we removed the 3' phosphates on the oligonucleotide digestion products to facilitate MS/MS sequencing of the longer oligonucleotides, which previously was shown to reduce the complexity of oligonucleotide MS/MS spectra by removing the 3'-phosphate loss fragmentation product ion and increasing the abundance of sequence informative c- and y- ions (Krivos et al. 2011). The digestion products were separated by hydrophilic interaction chromatography (HILIC) prior to detection and sequencing by high resolution tandem mass spectrometry. Despite ion pairing reversed phase chromatography (IP-RPLC) being the most common form of chromatography for bottom-up RNA sequencing, we employed HILIC with fully MS compatible mobile phases without the presence of instrument contaminating ion pair reagents.

As expected, the complete digestion of *S. cerevisiae* total tRNA using RNase T1 produced minimal sequence coverage (most tRNAs between 10-30% coverage), primarily due to the significant production of nonunique oligonucleotide digestion products

(**Figure 2A, 2B, and 3A, and Supplementary Table S1**). Comparatively, the folded tRNA RNase T1 digestions obtain significantly higher sequence coverages for the *S. cerevisiae* tRNA, where most tRNAs obtain between 60%-90% sequence coverage (**Table 1, Figure 2A, 2B, and 3A, and Supplementary Table S2)**. Notably, when the two datasets are utilized in tandem (unfolded + folded), the sequence coverage of most *S. cerevisiae* tRNAs is not improved further. As mentioned previously, the folded tRNA does not completely eliminate the production of complete RNase oligonucleotide digestion products. Thus, many of the digestion products detected in the complete RNase T1 digestion are subsequently redetected in the folded tRNA digestions. Additionally, the folded total tRNA RNase T1 digestions also produce longer digestion products that provide further sequence confidence for these regions. While LC-MS signal intensity can be distributed between multiple oligonucleotide digestion products that map back to the same location within a tRNA, folding tRNA prior to RNase digestions enables sequencing of areas that produce nonunique digestion products by complete digestions **(Figure 2A through 2D)**. Thus, in tandem characterization of unfolded and folded tRNAs is not required to maximize the sequence coverage of most tRNA by bottom-up RNA sequencing.

Our denaturing urea polyacrylamide gel electrophoresis (urea-PAGE) and LC-UV analyses suggest that RNase T1 digests tRNA in the three single stranded stem loop regions to produce oligonucleotide digestion fragments in 14-20 nt and > 30 nt ranges **(Figure 1B, 1C, and 1D)**. By LC-MS/MS, we confirmed this notion where the oligonucleotide digestion products enriched in the folded total tRNA RNase T1 digestions primarily extend between two neighboring stem loop regions **(Figure 2A and 2B)**. These longer digestion products enable the sequence of highly guanosine rich regions within the double stranded regions that would be missed by complete RNase T1 digestions. Despite producing longer oligonucleotide digestion products, the oligonucleotide fragments are readily sequenced using collision induced dissociation (CID) tandem mass spectrometry fragmentation and produce confident oligonucleotide MS/MS coverage maps **(Figure 3B through 3E and Supplemental Figures S5 to S8)**. While longer oligonucleotides (e.g., intact tRNAs and CRISPR oligonucleotides) require specialized fragmentation techniques and long scan times (minutes of spectral averaging) to produce adequate spectra, the

oligonucleotide digestion products remain in a length regime capable of sequencing on the time scales of a UHPLC chromatographic peak (milliseconds for confident MS/MS spectrum). Further, we found that RNase T1 can cleave within tRNA variable regions and at mismatched base paired sites **(Figure 2A and 2B)**, consistent with previous findings suggesting that these locations are more dynamic within the folded tRNA. Taken together, our results support that the stable tRNA secondary structure restrains RNase digestion primarily to single stranded regions within the tRNA, resulting in the production of longer and more specific digestion products that enhance bottom-up RNA sequencing.

To further increase total tRNA sequencing coverage, we used LC-MS/MS to sequence the products of an orthogonal digestion by RNase A. RNase A has been previously utilized to sequence purified individual tRNAs with up to 45% coverage (Yan et al. 2021). We find that complete digestion of total *S. cerevisiae* tRNA by RNase A results in minimal (0-22%) sequence coverage for any given tRNA **(Figure 3A, Table 1, and Supplementary Table S3)**. This is unsurprising given that RNase A cleaves at both pyrimidine residues, generating a complicated mixture of short, non-specific oligonucleotide digestion products. However, when RNase A cleaves fold *S. cerevisiae* total tRNA, the attainable sequence coverage is increased by 4-16% for 14 tRNAs **(Table 1 and Supplementary Table S4)**. Similar to RNase T1, the improved bottom-up RNA sequencing coverage results from the production of longer oligonucleotide digestions products from the cleavage solely at the single stranded stem loop regions. When compared in tandem to the complete and folded total tRNA RNase T1 digestions, RNase A digestions produce some orthogonality and improve the sequence coverage by 5-25% for over 15 *S. cerevisiae* tRNAs **(Table 1 and Figure 3A)**.

For most bottom-up RNA sequencing analyses, IP-RPLC is primarily used since it provides supreme chromatographic resolution and electrospray ionization (ESI) efficiency compared to HILIC (Apffel et al. 1997; Basiri et al. 2017). However, ion pairing reagents are known to contaminate liquid chromatographs and mass spectrometers (Ross et al. 2016), which limits these applications to designated negative mode instrumentation. Here, we utilize HILIC with fully ESI compatible ammonium acetate mobile phases and obtain good sequence coverage of *S. cerevisiae* total tRNA by bottom-up RNA

sequencing. However, full sequence coverage is not obtained in the folded RNase T1 and RNase A digestions, despite providing a longer oligonucleotide digestion pool. Specifically, we find that the lowest abundant tRNAs (e.g. Ser^{UGA}, Ser^{CGA}) generally report worse sequence coverages in folded total tRNA RNase digestions, likely resulting from ion suppressive coelution of oligonucleotide digestion products from higher abundance tRNAs that hinder detection.

HILIC struggles to adequately resolve longer oligonucleotide digestion products, likely resulting in ion suppression of co-eluting oligonucleotide digestion products that could provide additional sequencing for lower abundance tRNAs. Further, the poor ESI ionization efficiency of longer oligonucleotides further limits the detection of longer oligonucleotide digestion products. We find that LC-MS struggles to detect longer oligonucleotides using HILIC mobile phases despite being relatively abundant based on LC-UV signal **(Supplemental Figure S9)**. We believe that this methodology could be facilitated by the better chromatographic resolution and ESI sensitivities of IP-RPLC mobile phases or other improved separations. This is especially true for RNase A digestions, where most oligonucleotide digestion products are more than 30 nt in length **(Supplemental Figure S4)**. Until then, in tandem utilization of the orthogonal RNase T1 digestions and RNase A is recommended to maximize sequence coverage. Despite these limitations, we significantly improved sequence coverage obtainable for *S. cerevisiae* total tRNA by utilizing the intrinsic tRNA structure to enable the selective digestion of tRNAs by ribonucleases prior to bottom-up RNA sequencing.

We find that the folded total tRNA RNase digestions are highly reproducible in multiple replicate digestions **(Supplemental Figure S10)**, where 169 oligonucleotide digestion products out of 170 were detected in both folded total tRNA replicate digestions **(Supplemental Table S2)**. Further, folded total tRNA RNase T1 digestions are only modestly more variable than complete RNase T1 digestions, where the average coefficient of variation of LC-MS/MS peak areas between two digestion replicates is 19% and 13%, respectively **(Supplemental Tables S1 and S2)**. This suggests that the tRNA refolds into reproducible secondary structures, resulting in RNase cleavage at consistent available sites within the folded tRNA. This is supported by LC-MS/MS data where only

3’ phosphate oligonucleotide digestion products are produced during the folded tRNA digestions **(Supplemental Figure S3)**. Ribonuclease that produces 3’ phosphate digestion products go through a 2’3’-cyclic phosphate intermediate, which results in a mixture of 3’ phosphate and 2’3’-cyclic phosphates when RNA is partially digested (Vanhinsbergh et al. 2022). Since we only observe 3’ phosphates, we can ascertain that the RNase T1 and RNase A digestions of folded tRNA cleaves all available sites prior to full protection by remaining tRNA secondary structure of the nicked oligonucleotide fragments. This suggests that RNase T1 and RNase will produce consistent oligonucleotide digestion product pools presuming tRNA folds into consistent secondary structures during tRNA folding protocols.

Today, total tRNA sequencing is most commonly conducted using indirect next generation RNA sequencing (RNA-seq) methods that struggle to identify what modifications are present at specific sites within tRNA. Bottom-up RNA sequencing of total tRNA provides an attractive alternative that directly sequences and identifies modifications within an RNA strand. Here, we adapted well established bottom-up RNA sequencing pipelines by folding tRNA prior to enzymatic digestion, producing longer and more specific oligonucleotide digestion products by hindering digestion to tRNA single stranded stem loops. This alteration enables the direct total tRNA sequencing by LC-MS/MS with up to 97% **(Supplemental Table S5)** sequence coverage using well-characterized, commercially available enzymes. This work expands the current epitranscriptomic toolbox to comprehensively interrogate the molecular level consequences of the tRNA modifications landscape. While we apply this bottom-up RNA sequencing platform to confirm previously identified modified positions within *S. cerevisiae* total tRNA, this assay can be further implemented for *de novo* identification of previously undescribed modified sites. Particularly, this bottom-up RNA sequencing pipeline can be used in tandem with RNA-seq (Motorin and Marchand 2021; Watkins et al. 2022), direct Nanopore sequencing (DRS) (White and Hesselberth 2022; Thomas et al. 2021), and global ribonucleoside modification profiling (GRMP) (Jones et al. 2023a) to provide an overarching view of what modifications are present, where they are present, and how abundant the modifications are. Currently, the tRNA modification landscapes of many model organisms remain uncharacterized (e.g., *M. musculus* and *D. melanogaster*)

(Boccaletto et al. 2018) despite the increasing recognition that tRNA modifications play significant roles in cellular stress and disease (Suzuki 2021; Huber et al. 2019). Utilizing the bottom-up RNA sequencing approach developed here in tandem with current NGS, DRS, and GRMP pipelines will disencumber current limitations to directly identify what modifications are present at specific sites. Further, these approaches will enable the global characterization of how the tRNA modification landscape differs between tissues and is altered under cellular stress and disease. Together, this toolbox provides a comprehensive bioanalytical and biochemical analysis pipeline to undertake novel interrogations into the molecular level consequences and dynamics of the tRNA modification landscape.

Methods

Optimization of ribonuclease digestions of unfolded and folded total tRNAs

Folded tRNA RNase digestions were optimized with 75 µg of *S. cerevisiae* total tRNA (Sigma Aldrich) digested in a final reaction volume of 50 µL. For unfolded/complete tRNA digestions, the total tRNA was digestions with 100 U of RNase T1 per µg of RNA or 100 ng RNase A per µg of RNA at 37℃ for 1 hr in 220 mM ammonium acetate (unadjusted pH). Folded total tRNA was digested with RNase T1 at either 100 U/µg, 50 U/µg, or 25 U/µg at either 37℃, 30℃, or 25℃ for 1 hr. Prior to digestion, total tRNA was heat denatured at 95℃ for 10 min in 50 mM 2-(N-morpholino)ethanesulfonic acid (MES) pH 6.0 and 200 mM KCl (RNase T1) or 400 mM NaCl (RNase A). The denatured tRNA was transferred to a 37℃ heating block for 10 min. Subsequently, 2 M $MgCl_2$ was added to a final concentration of 20 mM $MgCl_2$ prior to heating at 37℃ for an additional 30 min. Either RNase T1 or RNase A were added prior to digestion at the corresponding temperature for 1 hr. The digestion was quenched with the addition of 50 µL acid phenol:chloroform:isoamyl alcohol (125:24:1; Sigma-Aldrich, USA; P1944) to denature the ribonucleases. The mixture was vortexed and centrifuged at 8,000 x g for 5 min. The aqueous layer was transferred to a separate clean tube.

RNA digestion products were visualized by both gel and LC-UV. For urea-PAGE analysis, 20 µL of the aqueous layer was removed and diluted with 1 volume of urea-PAGE denaturing loading dye (final concentration of 1X tris-borate-EDTA running buffer and 3.5 M urea with bromophenol blue and xylene cyanole). The mixture was heated at 95℃ for 15 min prior to separation on an 18 cm 20% urea PAGE gel run at constant power of 18 W with 1X TBE running buffer. Following, the gel was stained with methylene blue and destained with 18 MΩ water. The gels were imaged using a BioRad ChemiDoc MP Imaging System.

The RNase digestions were further characterized by LC-UV, where 5 µL injection of the digested total tRNA was separated with a Waters ACQUITY Premier BEH Amide VanGuard FIT column (1.7 µm 2.1 x 100 mm, 130Å) on an Agilent Infinity II 1290 Bio liquid chromatograph equipped with an Agilent 1290 II DA detector. Mobile phase A was 25 mM LC-MS grade ammonium acetate (unadjusted pH) with 2.5 µM medronic acid

(Agilent InfinityLab Deactivator Additive) in 100% water, and mobile phase B was 25 mM LC-MS grade ammonium acetate with 2.5 µM medronic acid in 80:20 acetonitrile:water (unadjusted pH). The flowrate was 250 µL/min and the column temperature was 55°C. The LC gradient is displayed in **Supplemental Table S6**.

Ribonuclease digestion of unfolded and folded total tRNA for LC-MS/MS analysis

For unfolded/complete digestions, 900 µg of *S. cerevisiae* total tRNA (Sigma-Aldrich) was digested by either 100 U/µg RNase T1 or 100 ng/µg RNase A in 220 mM ammonium acetate (unadjusted pH) at 37°C for 1 hr in 600 µL total volume. The digestions were quenched by the addition of 600 µL acid phenol:chloroform:isoamyl alcohol (125:24:1; Supelco; 77619). The mixture was vortexed and centrifuged at 8,000 x g for 5 min. The upper aqueous phase was washed with 600 µL chloroform, followed by vortexing and centrifugation at 8,000 x g for 2 min. The aqueous phase was transferred to a clean tube. To the resulting digested oligonucleotide mixture, quick calf intestinal phosphatase (CIP, NEB, USA) was added to a final concentration of 0.13 U/µg total tRNA and incubated for 1 hr at 25°C. The CIP was quenched by the addition of 600 µL acid phenol:chloroform:isoamyl alcohol (125:24:1; Supelco; 77619). The mixture was vortexed and centrifuged at 8,000 x g for 5 min. The upper aqueous phase was washed with 600 µL chloroform, followed by vortexing and centrifugation at 8,000 x g for 2 min. The upper aqueous phase (approximately 600 µL) was transferred to a clean tube prior to precipitation with 2 µL glycoblue, 65 µL 3 M NaOAc pH 5.2, and 2 mL ethanol.

Folded digestions were again accomplished using 900 µg of *S. cerevisiae* total tRNA was denatured at 95°C for 15 min in 50 mM MES pH 6.0 with 200 mM KCl (RNase T1) or 400 mM NaCl (RNase A) in 600 µL total volume. After denaturation, the digested total tRNA was heated for 37°C for 10 minutes prior to the addition of 6 µL 2 M $MgCl_2$. Following, the mixture was heated at 37°C for 30 min to allow the tRNA to fold. The resulting folded tRNA was digested with either 25 U/µg RNase T1 or 25 ng/µg RNase A at 25°C for 1 hr. The digestions were quenched by the addition of 600 µL acid phenol:chloroform:isoamyl alcohol (125:24:1; Supelco; 77619). The mixture was vortexed and centrifuged at 8,000 x g for 5 min. The upper aqueous phase was washed with 600

μL chloroform, followed by vortexing and centrifugation at 8,000 x g for 2 min. The aqueous phase was transferred to a clean tube. To the resulting digested oligonucleotide mixture, CIP was added to a final concentration of 0.13 U/μg total tRNA and incubated for 1 hr at 25℃. The CIP was quenched by the addition of 600 μL acid phenol:chloroform:isoamyl alcohol. The mixture was vortexed and centrifuged at 8,000 x g for 5 min. The upper aqueous phase was washed with 600 μL chloroform, followed by vortexing and centrifugation at 8,000 x g for 2 min. The upper aqueous phase (approximately 600 μL) was transferred to a clean tube prior to precipitation with 2 μL glycoblue, 65 μL 3 M NaOAc pH 5.2, and 2 mL ethanol.

Total tRNA partial digestions were performed with 75 mU of RNase T1 per μg of RNA for 30 minutes at 37℃. Following, the digestions were quenched with phenol:chloroform:isoamyl alcohol and washed with chloroform as described above. Prior to use, the phenol:chloroform:isoamyl was washed three separate times with 1 volume of water to remove excess sodium acetate that worsens HILIC chromatography. Each time, the upper aqueous phase was removed and replaced with 1 volume of fresh water. The washed lower organic phase was used for subsequent digestion quenching.

LC-MS/MS analysis of total tRNA digests

Prior to LC-MS/MS analysis, the complete and folded digestions were resuspended in 20 μL of 200 mM ammonium acetate (unadjusted pH), where 5 μL was injected onto to the column. The LC parameters (e.g., mobile phases, gradient, column temperature) are listed above. The LC was interfaced to a ThermoFisher Orbitrap Fusion Lumos mass spectrometer, where the spray voltage was -2.8 kV, the sheath gas was 35, the aux gas was 10, the sweep gas was 0, RF lens was 50%, the ion transfer tube temperature was 350℃, and the vaporizer temperature was 350℃. Data acquisition was performed using data dependent acquisition (DDA) with the Orbitrap used for both precursor and product ion scans at 60 K and 30 K resolution, respectively. MS1 scans were collected from 300 – 2000 m/z with a maximum injection time of 100 ms and normalized automatic gain control (AGC) target of 120%. The MS2 scans were collected from 150 – 2000 m/z with a maximum injection time of 200 ms and normalized automatic

gain control (AGC) target of 200%. Precursor ions with charge state between 2-6 with a signal intensity above 25,000 counts were selected for a fragmentation scan (maximum of five per cycle). Precursor ions were isolated with a 2 m/z isolation window and were fragmented using CID with a collision energy of 35% and activation time of 10 ms prior to analysis in the Orbitrap. Following fragmentation, the ion was excluded for 3 seconds before being selected for fragmentation again.

LC-MS/MS data was analyzed using ThermoFisher BioPharma Finder 5.1. *S. cerevisiae* tRNA sequences and modified positions were obtained from Modomics (Boccaletto et al. 2018), where modified sites were fixed at specific positions within each tRNA. *De novo* searching of modified positions was not performed. Oligonucleotide identifications were filtered to be within 10 ppm and greater than 85% confidence to be confirmed as a confident identification. The confidence score is a BioPharma Finder provided parameter that characterizes the similarity between a theoretical MS/MS spectrum to the actual MS/MS spectrum collected during analysis based on multiple parameters based on the characteristic fragmentation ions (mass accuracy, MS/MS ion distribution, modification neutral base loss). All identified oligonucleotides were manually inspected for proper monoisotopic mass deconvolution and quality MS/MS spectra. For N6-threonylcarbamoyladenosine (t^6A) containing oligonucleotides, confidence scores below 85% confidence were allowed; however, thorough characterization of the MS/MS spectra was performed. t^6A results in significant fragmentation within the modification, resulting a significant uninformative fragmentation ion that alters the BioPharma Finder quality score.

Author Information

Corresponding Author
Kristin Koutmou, 930 N University, Ann Arbor, MI 48109, kkoutmou@umich.edu, (734) 764-5650

ORCID
0000-0002-8811-1340 (J. D. Jones)
0009-0000-5358-7851 (K.M. Simcox)
0000-0003-2447-7471 (R. T. Kennedy)
0000-0002-7763-9262 (K. S. Koutmou)

Author Contributions

Joshua D. Jones: Conceptualization, Methodology, Investigation, Formal Analysis, Writing – Original Draft, Writing – Review & Editing, Visualization
Kaley M. Simcox: Methodology, Investigation, Formal Analysis, Writing – Review & Editing
Robert T. Kennedy: Writing – Review & Editing
Kristin S. Koutmou: Conceptualization, Writing – Review & Editing

Notes

The authors declare no competing financial interests.

Acknowledgements

We thank the following funding sources for their support: National Science Foundation (NSF CAREER 2045562 to K.S.K., GFRP to J.D.J., and NSF CHE 1904146 to R.T.K.) and the Research Corporation for Science Advancement (Cottrell Scholar award to K.S.K.). Research reported in this publication was supported by instrumentation at the University of Michigan Chemistry Mass Spectrometry Core, which purchased with funds from the Office of the Director, National Institutes of Health under Award Number S10OD021619. We thank Dr. Daniel Eyler and Dr. Christopher Rohlman for their helpful comments on the manuscript.

Figures:

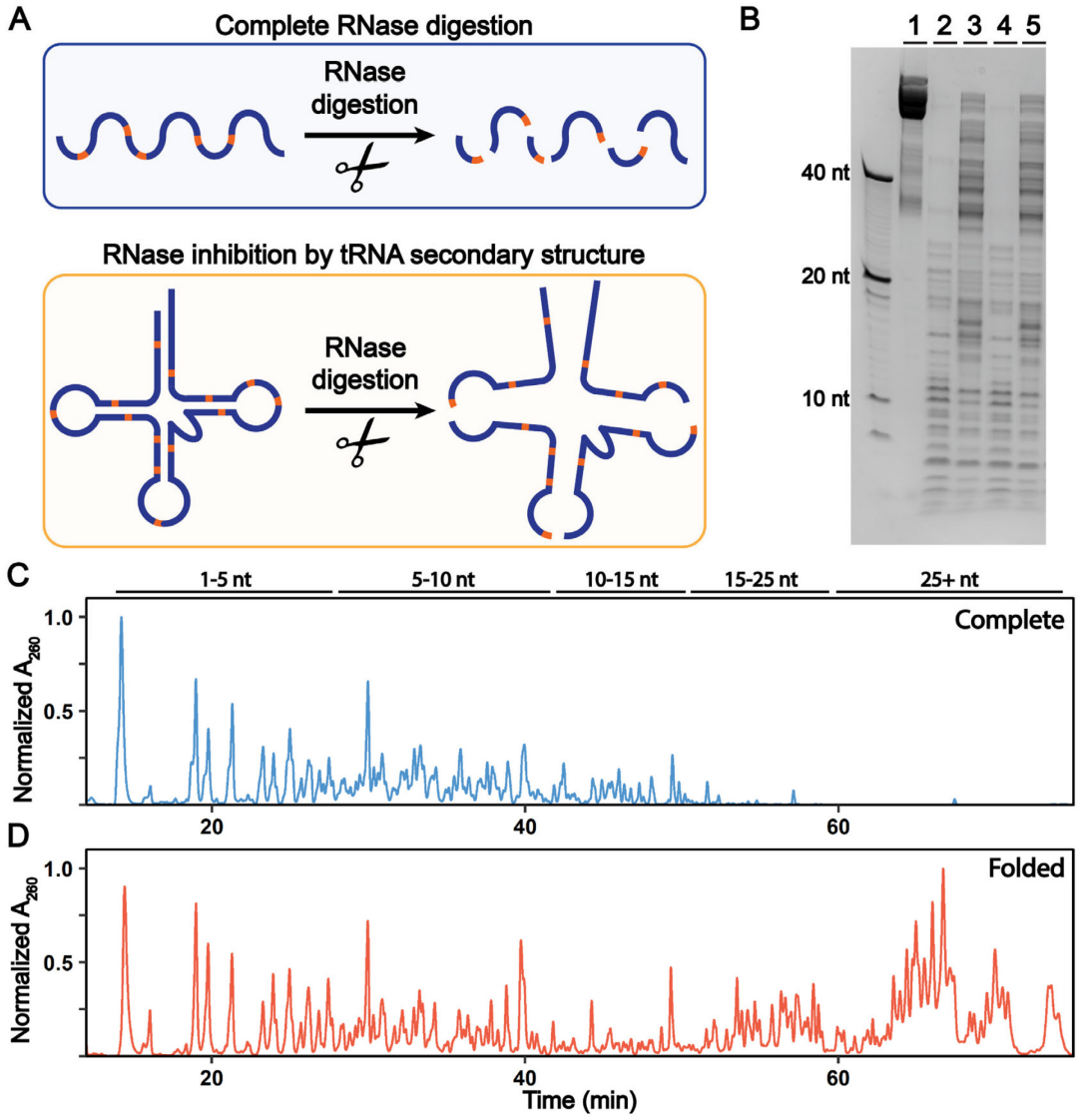

Figure 1: tRNA secondary structure protects against digestion by single stranded specific RNase T1. (A) For complete digestion, single stranded specific RNases digest at every cleavage site (top panel), while we predict that tRNA secondary structure will restrict digestion to only available motifs in the single stranded stem loops (bottom panel). **(B)** Denaturing urea-PAGE gel electrophoresis displaying the oligonucleotide digestion products produced from the complete and folded RNase T1 digestions with 25 U/μg RNase T1 at 25℃ with the following digestion conditions: Lane 1: undigested *S. cerevisiae* total tRNA; lane 2: complete digestion in NH_4OAc; lane 3: digestion in NH_4OAc + 20 mM $MgCl_2$; lane 4: heat denatured tRNA in MES + KCl; lane 5: MES + KCl + $MgCl_2$. **(C)** LC-UV of total tRNA complete RNase T1 digestion (lane 2 of panel B). **(D)** LC-UV of folded total tRNA RNase T1 digestion (lane 5 of panel B). Comparison of **(C)** and **(D)** reveals that digestion of folded total tRNAs leads to shifts the distribution of RNA fragments to longer lengths.

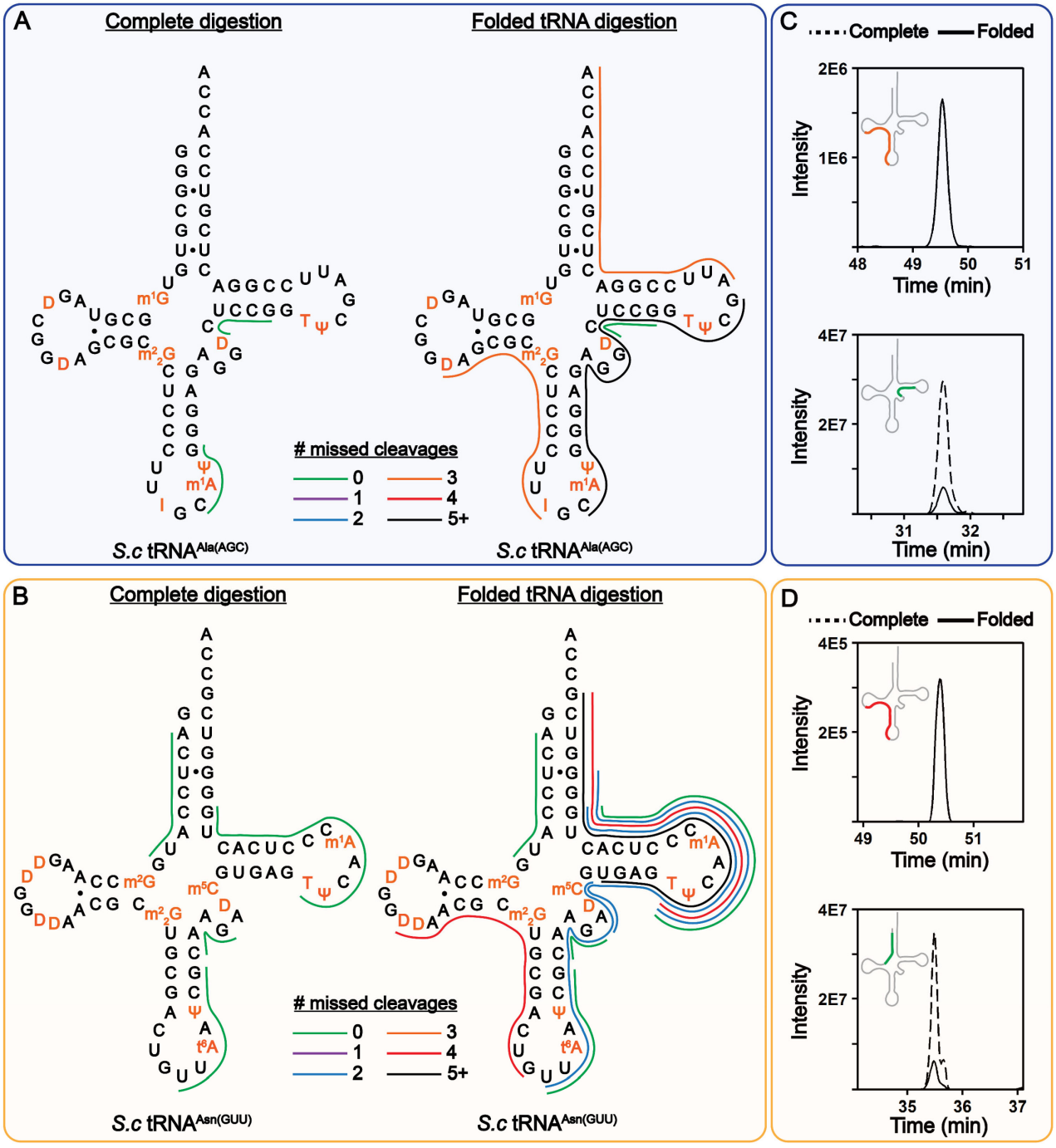

Figure 2: Bottom-up sequencing of *S. cerevisiae* tRNA$^{Ala(AGC)}$ and tRNA$^{Asn(GUU)}$ in total tRNA pool. The detected oligonucleotide digestion products for **(A)** tRNA$^{Ala(AGC)}$ and **(B)** tRNA$^{Asn(GUU)}$ in complete digestions and folded tRNA digestions by RNase T1. The colors correspond to the number of missed cleavages in the detected RNA fragment. Extracted ion chromatograms (EICs) for two oligonucleotides detected in **(C)** tRNA$^{Ala(AGC)}$ and **(D)** tRNA$^{Asn(GUU)}$ displaying the enrichment of longer RNA digestion products in the folded tRNA RNase T1 digestions.

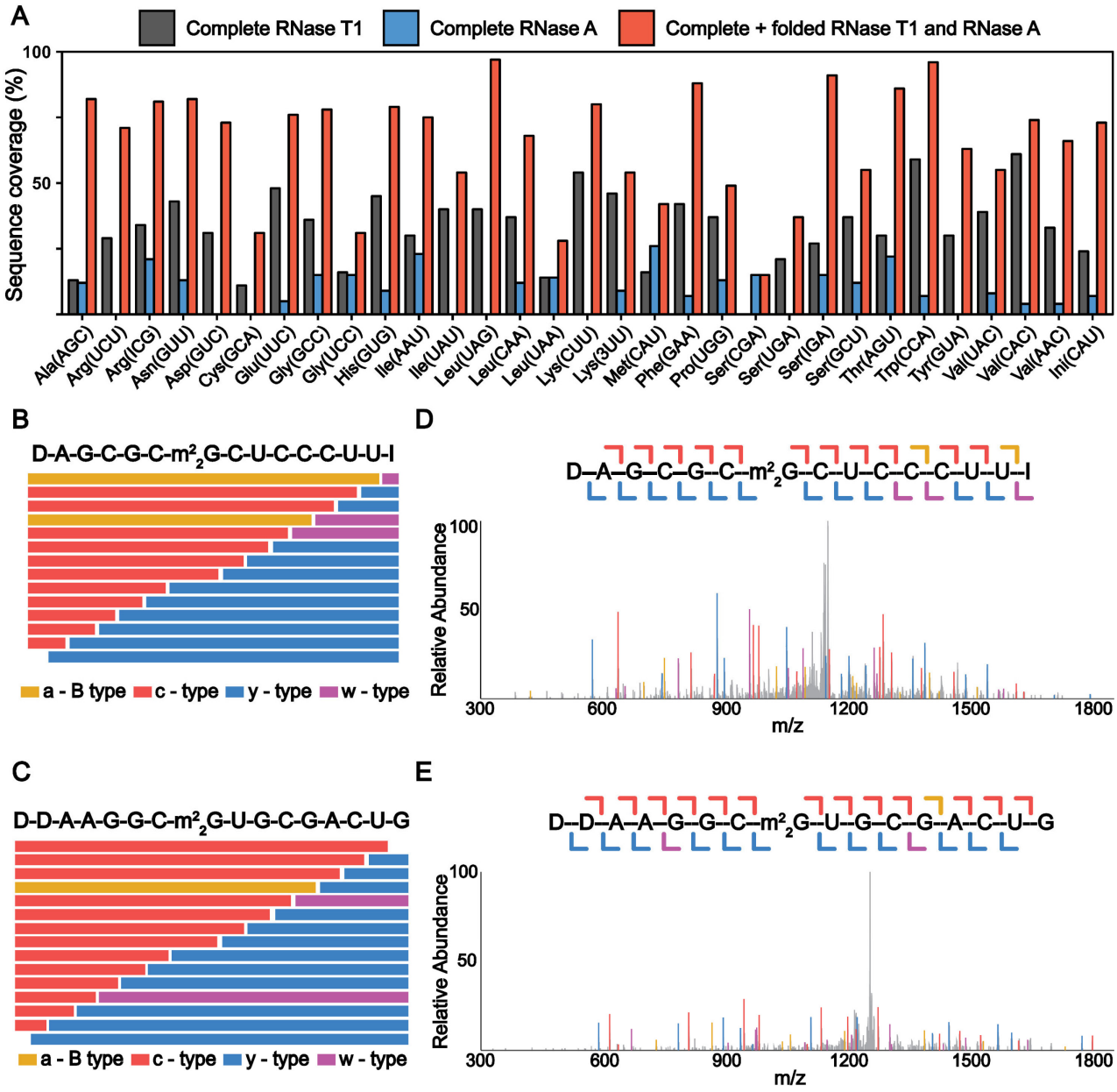

Figure 3: MS/MS sequencing of folded total tRNA oligonucleotide digestion products. (A) The sequence coverage for each individual tRNA from a complete RNase T1 digestion (grey), complete RNase A digestion (blue), and a combination of complete and folded digestions using RNase T1 and RNase A (red). The sequence coverage consists of solely unique oligonucleotides detected with high confidence by BioPharma Finder. Data displayed in figure can be found in Table 1. **(B)** The oligonucleotide MS/MS coverage map for DAGCGCm$^2_2$GCUCCCUUI (1179.4158 m/z) for tRNA$^{Ala(AGC)}$ oligonucleotide digestion product produces from **(D)** sequence informative fragmentation ions detected in MS/MS spectra. **(C)** The oligonucleotide MS/MS coverage map for DDAAGGCm$^2_2$GUGCGACUG (1291.6879 m/z) for tRNA$^{Asn(GUU)}$ oligonucleotide digestion product produces from **(E)** sequence informative fragmentation ions detected in MS/MS spectrum. The color of the oligonucleotide MS/MS coverage map bars and labeled ions detected in MS/MS spectra correspond to the type of oligonucleotide MS/MS ion detected. The most

abundant MS/MS fragment ion of the a-B/c- and w-/y- MS/MS ion type pairs was depicted in **(B)** and **(C)**, even if both ions are present.

Table 1: Observed sequence coverage of *S. cerevisiae* total tRNA by complete digestions and folded tRNA digestions by RNase T1 and RNase A. For tRNAs containing multiple sequences for a single tRNA isoacceptor (e.g., *S. cerevisiae* $tRNA^{His(GUG)}$), a single sequence was utilized for sequence coverage analysis to reduce production of non-unique oligonucleotide digestion products detected.

tRNA	Sequence coverage (%)						
	Unfolded RNase T1	Folded RNase T1	Unfolded + folded RNase T1	Unfolded RNase A	Folded RNase A	Unfolded + folded RNase A	All four conditions
Ala (AGC)	13	74	74	12	38	38	82
Arg (UCU)	29	63	63	0	35	35	71
Arg (ICG)	34	80	80	21	67	67	81
Asn (GUU)	43	82	82	13	0	13	82
Asp (GUC)	31	56	56	0	61	61	73
Cys (GCA)	11	31	31	0	0	0	31
Glu (UUC)	48	61	61	5	43	48	76
Gly (GCC)	36	70	78	15	33	33	78
Gly (UCC)	16	16	16	15	7	15	31
His (GUG)	45	66	71	9	9	9	79
Ile (AAU)	30	74	74	23	8	23	75
Ile (UAU)	40	47	54	0	0	0	54
Leu (UAG)	40	97	97	0	5	5	97
Leu (CAA)	37	62	62	12	37	37	68
Leu (UAA)	14	14	14	14	0	14	28
Lys (CUU)	54	72	72	0	20	20	80
Lys (3UU)	46	17	46	9	0	9	54
Met (CAU)	16	16	16	26	34	34	42
Phe (GAA)	42	49	65	7	21	28	88
Pro (UGG)	37	21	37	13	0	13	49
Ser (CGA)	0	0	0	15	0	15	15
Ser (UGA)	21	20	28	0	18	18	37
Ser (IGA)	27	72	80	15	54	54	91
Ser (GCU)	37	46	52	12	40	40	55
Thr (AGU)	30	84	84	22	37	38	86
Trp (CCA)	59	84	84	7	17	24	96
Tyr (GUA)	30	45	45	0	22	22	63
Val (UAC)	39	55	55	8	0	8	55
Val (CAC)	61	50	72	4	0	4	74
Val (AAC)	33	56	62	4	0	4	66
Ini (CAU)	24	72	72	7	0	7	73

References

Adams A, Lindahl T, Fresco JR. 1967. Conformational differences between the biologically active and inactive forms of a transfer ribonucleic acid. *Proceedings of the National Academy of Sciences* **57**: 1684–1691.

Addepalli B, Lesner NP, Limbach PA. 2015. Detection of RNA nucleoside modifications with the uridine-specific ribonuclease MC1 from Momordica charantia. *RNA* **21**: 1746–1756.

Addepalli B, Limbach PA. 2016. Pseudouridine in the Anticodon of Escherichia coli tRNATyr(QΨA) Is Catalyzed by the Dual Specificity Enzyme RluF. *J Biol Chem* **291**: 22327–22337.

Addepalli B, Venus S, Thakur P, Limbach PA. 2017. Novel ribonuclease activity of cusativin from Cucumis sativus for mapping nucleoside modifications in RNA. *Anal Bioanal Chem* **409**: 5645–5654.

Alings F, Sarin LP, Fufezan C, Drexler HCA, Leidel SA. 2015. An evolutionary approach uncovers a diverse response of tRNA 2-thiolation to elevated temperatures in yeast. *RNA* **21**: 202–212.

Apffel A, Chakel JA, Fischer S, Lichtenwalter K, Hancock WS. 1997. Analysis of Oligonucleotides by HPLC−Electrospray Ionization Mass Spectrometry. *Anal Chem* **69**: 1320–1325.

Asano K, Suzuki T, Saito A, Wei F-Y, Ikeuchi Y, Numata T, Tanaka R, Yamane Y, Yamamoto T, Goto T, et al. 2018. Metabolic and chemical regulation of tRNA modification associated with taurine deficiency and human disease. *Nucleic Acids Res* **46**: 1565–1583.

Ausubel FM, ed. 1987. *Current protocols in molecular biology*. Greene Pub. Associates ; J. Wiley, order fulfillment, Brooklyn, N.Y. : Media, Pa.

Basiri B, van Hattum H, van Dongen WD, Murph MM, Bartlett MG. 2017. The role of fluorinated alcohols as mobile phase modifiers for LC-MS analysis of oligonucleotides. *J Am Soc Mass Spectrom* **28**: 190–199.

Boccaletto P, Machnicka MA, Purta E, Piątkowski P, Bagiński B, Wirecki TK, de Crécy-Lagard V, Ross R, Limbach PA, Kotter A, et al. 2018. MODOMICS: a database of RNA modification pathways. 2017 update. *Nucleic Acids Res* **46**: D303–D307.

Cao X, Limbach PA. 2015. Enhanced Detection of Post-Transcriptional Modifications Using a Mass-Exclusion List Strategy for RNA Modification Mapping by LC-MS/MS. *Anal Chem* **87**: 8433–8440.

Chan CTY, Dyavaiah M, DeMott MS, Taghizadeh K, Dedon PC, Begley TJ. 2010. A Quantitative Systems Approach Reveals Dynamic Control of tRNA Modifications during Cellular Stress. *PLOS Genetics* **6**: e1001247.

Chan CTY, Pang YLJ, Deng W, Babu IR, Dyavaiah M, Begley TJ, Dedon PC. 2012. Reprogramming of tRNA modifications controls the oxidative stress response by codon-biased translation of proteins. *Nat Commun* **3**: 937.

Crittenden CM, Lanzillotti MB, Chen B. 2023. Top-Down Mass Spectrometry of Synthetic Single Guide Ribonucleic Acids Enabled by Facile Sample Clean-Up. *Anal Chem* **95**: 3180–3186.

de Crécy-Lagard V, Ross RL, Jaroch M, Marchand V, Eisenhart C, Brégeon D, Motorin Y, Limbach PA. 2020. Survey and Validation of tRNA Modifications and Their Corresponding Genes in Bacillus subtilis sp Subtilis Strain 168. *Biomolecules* **10**: 977.

Donis-Keller H, Maxam AM, Gilbert W. 1977. Mapping adenines, guanines, and pyrimidines in RNA. *Nucleic Acids Research* **4**: 2527–2538.

Goyon A, Nguyen D, Boulanouar S, Yehl P, Zhang K. 2022. Characterization of Impurities in Therapeutic RNAs at the Single Nucleotide Level. *Anal Chem* **94**: 16960–16966.

Goyon A, Scott B, Kurita K, Crittenden CM, Shaw D, Lin A, Yehl P, Zhang K. 2021. Full Sequencing of CRISPR/Cas9 Single Guide RNA (sgRNA) via Parallel Ribonuclease Digestions and Hydrophilic Interaction Liquid Chromatography–High-Resolution Mass Spectrometry Analysis. *Anal Chem* **93**: 14792–14801.

Hagelskamp F, Borland K, Ramos J, Hendrick AG, Fu D, Kellner S. 2020. Broadly applicable oligonucleotide mass spectrometry for the analysis of RNA writers and erasers in vitro. *Nucleic Acids Res* **48**: e41–e41.

Huber SM, Leonardi A, Dedon PC, Begley TJ. 2019. The Versatile Roles of the tRNA Epitranscriptome during Cellular Responses to Toxic Exposures and Environmental Stress. *Toxics* **7**: 17.

Ishida K, Kunibayashi T, Tomikawa C, Ochi A, Kanai T, Hirata A, Iwashita C, Hori H. 2011. Pseudouridine at position 55 in tRNA controls the contents of other modified nucleotides for low-temperature adaptation in the extreme-thermophilic eubacterium Thermus thermophilus. *Nucleic Acids Research* **39**: 2304–2318.

Jackman JE, Alfonzo JD. 2013. Transfer RNA modifications: nature's combinatorial chemistry playground. *Wiley Interdisciplinary Reviews: RNA* **4**: 35–48.

Jiang T, Yu N, Kim J, Murgo J-R, Kissai M, Ravichandran K, Miracco EJ, Presnyak V, Hua S. 2019. Oligonucleotide Sequence Mapping of Large Therapeutic mRNAs via Parallel Ribonuclease Digestions and LC-MS/MS. *Anal Chem* **91**: 8500–8506.

Jones JD, Franco M, Smith T, Snyder LR, Anders AG, Ruotolo BT, Kennedy RT, Koutmou KS. 2023a. Methylated guanosine and uridine modifications in S. cerevisiae mRNAs modulate translation elongation. *RSC Chem Biol*. https://pubs.rsc.org/en/content/articlelanding/2023/cb/d2cb00229a (Accessed March 8, 2023).

Jones JD, Grassmyer KT, Kennedy RT, Koutmou KS, Maloney TD. 2023b. Nuclease P1 Digestion for Bottom-Up RNA Sequencing of Modified siRNA Therapeutics. *Anal Chem* **95**: 4404–4411.

Jones JD, Monroe J, Koutmou KS. 2020. A molecular-level perspective on the frequency, distribution, and consequences of messenger RNA modifications. *WIREs RNA* **11**: e1586.

Jora M, Lobue PA, Ross RL, Williams B, Addepalli B. 2019. Detection of ribonucleoside modifications by liquid chromatography coupled with mass spectrometry. *Biochimica et Biophysica Acta (BBA) - Gene Regulatory Mechanisms* **1862**: 280–290.

Kimura S, Dedon PC, Waldor MK. 2020. Comparative tRNA sequencing and RNA mass spectrometry for surveying tRNA modifications. *Nat Chem Biol* **16**: 964–972.

Kowalak JA, Pomerantz SC, Crain PF, McCloskey JA. 1993. A novel method for the determination of post-transcriptional modification in RNA by mass spectrometry. *Nucleic Acids Res* **21**: 4577–4585.

Krivos KL, Addepalli B, Limbach PA. 2011. Removal of 3'-phosphate group by bacterial alkaline phosphatase improves oligonucleotide sequence coverage of RNase digestion products analyzed by collision-induced dissociation mass spectrometry. *Rapid Communications in Mass Spectrometry* **25**: 3609–3616.

Lockard RE, Kumar A. 1981. Mapping tRNA structure in solution using double-strand-specific ribonuclease V1 from cobra venom. *Nucleic Acids Res* **9**: 5125–5140.

McCown PJ, Ruszkowska A, Kunkler CN, Breger K, Hulewicz JP, Wang MC, Springer NA, Brown JA. 2020. Naturally occurring modified ribonucleosides. *WIREs RNA* **11**: e1595.

Motorin Y, Marchand V. 2021. Analysis of RNA Modifications by Second- and Third-Generation Deep Sequencing: 2020 Update. *Genes (Basel)* **12**: 278.

Ohira T, Minowa K, Sugiyama K, Yamashita S, Sakaguchi Y, Miyauchi K, Noguchi R, Kaneko A, Orita I, Fukui T, et al. 2022. Reversible RNA phosphorylation stabilizes tRNA for cellular thermotolerance. *Nature* **605**: 372–379.

Pomerantz SC, McCloskey JA. 2005. Detection of the common RNA nucleoside pseudouridine in mixtures of oligonucleotides by mass spectrometry. *Anal Chem* **77**: 4687–97.

Popova AM, Williamson JR. 2014. Quantitative analysis of rRNA modifications using stable isotope labeling and mass spectrometry. *J Am Chem Soc* **136**: 2058–2069.

Puri P, Wetzel C, Saffert P, Gaston KW, Russell SP, Cordero Varela JA, van der Vlies P, Zhang G, Limbach PA, Ignatova Z, et al. 2014. Systematic identification of tRNAome and its dynamics in Lactococcus lactis. *Mol Microbiol* **93**: 944–956.

Ross R, Cao X, Yu N, Limbach PA. 2016. Sequence mapping of transfer RNA chemical modifications by liquid chromatography tandem mass spectrometry. *Methods* **107**: 73–8.

Schauss J, Kundu A, Fingerhut BP, Elsaesser T. 2021. Magnesium Contact Ions Stabilize the Tertiary Structure of Transfer RNA: Electrostatics Mapped by Two-Dimensional Infrared Spectra and Theoretical Simulations. *J Phys Chem B* **125**: 740–747.

Suzuki T. 2021. The expanding world of tRNA modifications and their disease relevance. *Nat Rev Mol Cell Biol* **22**: 375–392.

Suzuki T, Suzuki T. 2007. Chaplet column chromatography: isolation of a large set of individual RNAs in a single step. *Meth Enzymol* **425**: 231–239.

Suzuki T, Yashiro Y, Kikuchi I, Ishigami Y, Saito H, Matsuzawa I, Okada S, Mito M, Iwasaki S, Ma D, et al. 2020. Complete chemical structures of human mitochondrial tRNAs. *Nat Commun* **11**: 4269.

Taoka M, Nobe Y, Hori M, Takeuchi A, Masaki S, Yamauchi Y, Nakayama H, Takahashi N, Isobe T. 2015. A mass spectrometry-based method for comprehensive quantitative determination of post-transcriptional RNA modifications: the complete chemical structure of Schizosaccharomyces pombe ribosomal RNAs. *Nucleic Acids Res* **43**: e115.

Taoka M, Nobe Y, Yamaki Y, Sato K, Ishikawa H, Izumikawa K, Yamauchi Y, Hirota K, Nakayama H, Takahashi N, et al. 2018. Landscape of the complete RNA chemical modifications in the human 80S ribosome. *Nucleic Acids Res* **46**: 9289–9298.

Taoka M, Nobe Y, Yamaki Y, Yamauchi Y, Ishikawa H, Takahashi N, Nakayama H, Isobe T. 2016. The complete chemical structure of Saccharomyces cerevisiae rRNA: partial pseudouridylation of U2345 in 25S rRNA by snoRNA snR9. *Nucleic Acids Res* **44**: 8951–8961.

Taucher M, Breuker K. 2012. Characterization of Modified RNA by Top-Down Mass Spectrometry. *Angewandte Chemie International Edition* **51**: 11289–11292.

Taucher M, Breuker K. 2010. Top-down mass spectrometry for sequencing of larger (up to 61 nt) RNA by CAD and EDD. *J Am Soc Mass Spectrom* **21**: 918–929.

Thakur P, Estevez M, Lobue PA, Limbach PA, Addepalli B. 2020. Improved RNA modification mapping of cellular non-coding RNAs using C- and U-specific RNases. *Analyst* **145**: 816–827.

Thomas NK, Poodari VC, Jain M, Olsen HE, Akeson M, Abu-Shumays RL. 2021. Direct Nanopore Sequencing of Individual Full Length tRNA Strands. *ACS Nano* **15**: 16642–16653.

Vanhinsbergh CJ, Criscuolo A, Sutton JN, Murphy K, Williamson AJK, Cook K, Dickman MJ. 2022. Characterization and Sequence Mapping of Large RNA and mRNA Therapeutics Using Mass Spectrometry. *Anal Chem* **94**: 7339–7349.

Watanabe K, Miyagawa R, Tomikawa C, Mizuno R, Takahashi A, Hori H, Ijiri K. 2013. Degradation of initiator tRNA Met by Xrn1/2 via its accumulation in the nucleus of heat-treated HeLa cells. *Nucleic Acids Research* **41**: 4671–4685.

Watkins CP, Zhang W, Wylder AC, Katanski CD, Pan T. 2022. A multiplex platform for small RNA sequencing elucidates multifaceted tRNA stress response and translational regulation. *Nat Commun* **13**: 2491.

Wein S, Andrews B, Sachsenberg T, Santos-Rosa H, Kohlbacher O, Kouzarides T, Garcia BA, Weisser H. 2020. A computational platform for high-throughput analysis of RNA sequences and modifications by mass spectrometry. *Nature Communications* **11**: 1–12.

Wetzel C, Limbach PA. 2013. The global identification of tRNA isoacceptors by targeted tandem mass spectrometry. *Analyst* **138**: 6063–6072.

White LK, Hesselberth JR. 2022. Modification mapping by nanopore sequencing. *Frontiers in Genetics* **13**. https://www.frontiersin.org/articles/10.3389/fgene.2022.1037134 (Accessed January 17, 2023).

Wurst RM, Vournakis JN, Maxam AM. 1978. Structure mapping of 5'-32P-labeled RNA with S1 nuclease. *Biochemistry* **17**: 4493–4499.

Yamagami R, Sieg JP, Assmann SM, Bevilacqua PC. 2022. Genome-wide analysis of the in vivo tRNA structurome reveals RNA structural and modification dynamics under heat stress. *Proceedings of the National Academy of Sciences* **119**: e2201237119.

Yan T-M, Pan Y, Yu M-L, Hu K, Cao K-Y, Jiang Z-H. 2021. Full-Range Profiling of tRNA Modifications Using LC–MS/MS at Single-Base Resolution through a Site-Specific Cleavage Strategy. *Anal Chem* **93**: 1423–1432.

Yoluç Y, van de Logt E, Kellner-Kaiser S. 2021. The Stress-Dependent Dynamics of Saccharomyces cerevisiae tRNA and rRNA Modification Profiles. *Genes (Basel)* **12**: 1344.

Yu N, Jora M, Solivio B, Thakur P, Acevedo-Rocha CG, Randau L, de Crécy-Lagard V, Addepalli B, Limbach PA. 2019. tRNA Modification Profiles and Codon-Decoding Strategies in Methanocaldococcus jannaschii. *Journal of Bacteriology* **201**: e00690-18.

Zhang W, Foo M, Eren AM, Pan T. 2022. tRNA modification dynamics from individual organisms to metaepitranscriptomics of microbiomes. *Molecular Cell* **82**: 891–906.

Direct sequencing of total *S. cerevisiae* tRNAs by LC-MS/MS

Joshua D Jones, Kaley M Simcox, Robert T Kennedy, et al.

RNA published online May 11, 2023 originally published online May 11, 2023
Access the most recent version at doi:10.1261/rna.079656.123